J. Integr. Sci. Technol. 2025, 13(2), 1027

Journal of Integrated
SCIENCE & TECHNOLOGY

Classification of Celiac disease using ensemble SMOTE-RF approach

Nisha,* Prachi Chaudhary

Department of Electronics and Communication Engineering, DCR University of Science and Technology, Murthal, Haryana, India

Submitted on: 15-Jul-2024, Accepted and Published on: 03-Sep-2024

Article

ABSTRACT

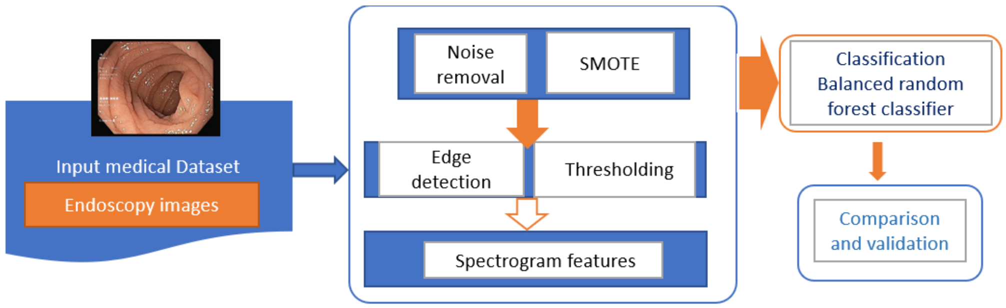

There are emerging challenges in the medical field as artificial intelligence is being introduced for automated detection of different diseases including celiac disease (CD). Manual interpretation is time time-consuming task performed by endoscopists whereas experience plays a key role in figuring out the abnormal region. The endoscopy images are processed with automated detection as their results are promising in terms of presence and non-presence of the disease. Initially, fastNLmeans denoising enabled pre-processing with Synthetic Minority Oversampling Technique (SMOTE) is utilized for mitigating the effect of the noise and for increasing the minority class images. For effective automatic classification, segmentation is a crucial step in image processing. Then, the Sobel operator with Multilevel Otsu thresholding is used as a segmentation step to reduce the complexity of the image. Image spatial features are extracted using a hybrid approach of discrete wavelet transform and high-order spectra (HOS). Thereafter, the Balanced random forest classifier is implemented to classify images as normal and abnormal. This model achieves remarkable performance with an accuracy of 89.41%, precision of 94.23%, recall of 89.09%, and F1 score of 91.58%. This approach validates the results with the help of endoscopists to prove its efficacy. These results outperform by imparting a high value of precision and F1 score.

Keywords: Celiac disease, SMOTE, Sobel Operator, DWT-HOS, Balanced random forest classifier

INTRODUCTION

Celiac disease (CD) is a dangerous public health issue worldwide. The CD is an autoimmune disorder triggered by taking a gluten-free diet that affects the small intestine villi structure. This results in malabsorption in children due to inflammation in the intestine.[1] Endoscopy is the safest and most frequent procedure performed for examining the GI tract as it does not contain any radiation. Our GI organs are very soft tissues irrespective of bone. X-rays can not be used to examine these soft tissues and organs. So, endoscopy is used for taking clear pictures without any radiation. It is embedded with a tiny camera and one light-emitting source attached to its other end.

*Corresponding Author: Nisha, DCRUST, Murthal, Haryana, India
Email: nishadalal.vce@gmail.com

Cite as: *J. Integr. Sci. Technol., 2025, 13(2), 1027.*
URN: NBN: sciencein.jist.2025.v13.1027
DOI: 10.62110/sciencein.jist. 2025.v13.1027

The prevalence of the disease is 1.4 % of the total world population and it varies from country to country due to changes in the environment and diet of the people.[2,3] England has reported half the cases than Scotland but the cases are still undiagnosed due to asymptotic behavior, which is difficult and not noticed during the inspection.[4,5] It is emerging in many Asian countries after Europe.[6,7] Earlier it was recognized in only children but it affects all age groups and genders including males and females.[8] Early detection is possible if we educate the people about the symptoms and prefer endoscopy for a positive serology test. The warning signs like weight loss, skin rashes, constipation, bloating, and growth reduction of the disease should be discussed with the public, nurses, and healthcare persons for early diagnosis to prevent cancer in the intestine. This disease is noticed in age groups greater than 40 years as the symptoms are not recognized at the initial stage. During the EGD procedure the markers are checked for damaged villi structure of the intestine manually,[9] This procedure however takes time to confirm due to its heterogeneous nature. Studying the nature of biopsy, and endoscopy images is also very challenging,[10] and sometimes orientation and preparation of biopsies is also not good.

The loss of folds may be due to age in adults (>60) which could misinterpret the results. The well-experienced endoscopist may experience interobserver variation during image explication. So, there is a need to explore a method with high sensitivity and accuracy to achieve full automated detection. Here, we focused on implementing a machine learning algorithm for the detection of villous atrophy in the small intestine duodenum part. So, a scientific tool is necessary for diagnosis at an early stage. Although blood tests have high accuracy they can not taken as the final decision so, an endoscopy is performed for a second opinion for checking other GI conditions also other than celiac. For training and research fellows, the automated system may benefit as visual detection needs supervision.[10] The markers are sometimes missing during EGD procedure in almost 23% of cases but villous atrophy is seen in other diseases and elderly cases so it does not confirm the presence of the disease. In that case, histopathological slides and serology testing confirm the presence of disease.[11]

For checking endoscopic markers and structure of folds remarkable growth in results can be seen with machine learning algorithms.[12] Easy and difficult types of images are chosen for classification for high performance. These methods have seen remarkable growth in medical imaging also.[13] Some statistical features are also observed with it which are not discoverable in manual inspection. Machine learning (ML) is a procedure of giving knowledge to the computer so that it can solve problems using its expertise.[14] It is cheap, fast, and takes less computation time for solving the data than human beings. As the human eye is susceptible to error, the correlation between images for large datasets is analyzed with ML. The results of ML are based on the combination of various algorithms based on the steps followed to deliver a conclusion.[15] This study focuses on classifying celiac disease endoscopy images as normal and abnormal using the most common ML algorithms and the effectiveness of the ML is identified by attaining high efficiency for a real dataset in classification and medical diagnosis.

WORKFLOW DESIGN

The designed framework is comprised of four parts: the first step is medical data acquisition for analysis. In the next step image processing techniques of preprocessing for noise removal and oversampling using SMOTE, segmentation to extract regions of interest, and extracting features using some feature extraction method. In the third step classification is done using a machine learning algorithm with the help of a cost-effective and time-saving balanced random forest classifier. To diagnose and validate the results in the fourth stage results are validated with an endoscopist. All the steps are processed using Python 3.11.3 on an Intel core i5 8th-generation processor with 64GB RAM and Windows 10. Figure 1 shows the workflow for the designed framework.

LITERATURE REVIEW

In recent years, various studies have been done on the diagnosis of celiac disease using machine learning and deep learning methods. Deep learning methods are used nowadays with high accuracy for the detection of colorectal polyps during colonoscopy as well as other GI disorders. However, these deep learning methods require large datasets and are complex to implement. The duodenum part is mostly overlooked as this is a landmark set for taking images for analysis.[16] There is a need to enhance awareness among endoscopists to carefully examine the duodenum part for the villous atrophy marker. The patient can avoid biopsy procedures by adopting computer-based diagnosis but they need to go through upper endoscopy. The AI algorithms provide high speed concerning complex algorithms used in capsule endoscopy.[17] Related work with its findings is listed in Table 1.

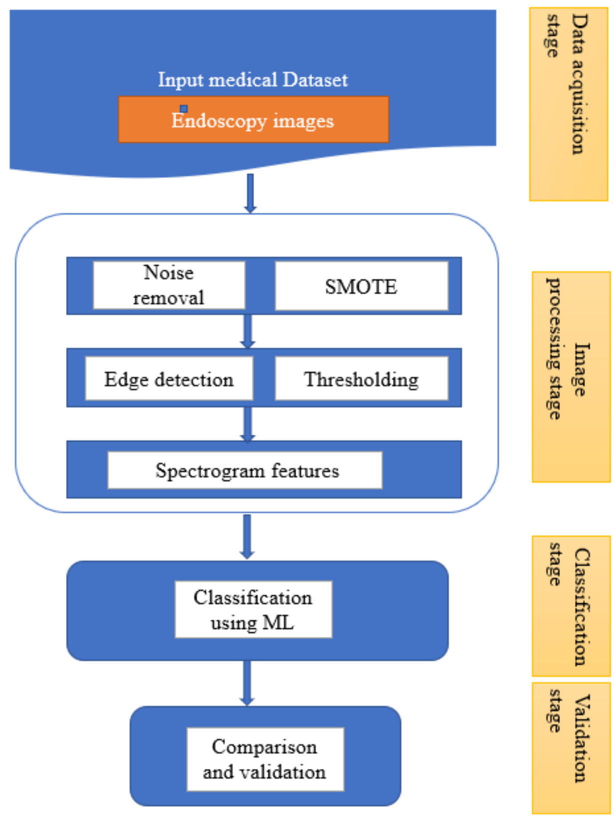

Figure 1: Detailed representation of designed framework

For studying biopsy images, an automated approach with machine learning was first used with steerable pyramid transform achieving an accuracy of 88.89%.[18] GoogleNet achieved 100% accuracy for video capsule images.[19] For basis images, the sensitivity of 84.6% and specificity of 92.3% are achieved for average of all basis images.[20] For breast cancer, random forest algorithm achieves 100% accuracy on the initial dataset and 99.30% on the minimal dataset.[21] The BCSE module on videocapsule images achieves an accuracy of 95.94%.[22] Daisy descriptor with PSO achieves 89.82% accuracy.[23] The SVM classification on endoscopy images achieves 92.0% accuracy.[24] Some studies show that the ensemble random forest algorithm is suitable for the detection of various diseases like heart disease with an accuracy of 83.85%,[25] Alzheimer's disease.[26] So, in this study, a Balanced Random forest classifier with tuned hyperparameters is used for the diagnosis of CD.

Table 1. Analysis of literature reports

Reference	Description	Source	Validation	Finding
Scheppach et al 2023 [10]	ResNet 18 was used	Endoscopy images 1704 training images 349 external testing images	5 fold cross validation	Internal cross validation achieved senitivity 82%, Specificity 85%, Accuracy 84% External test dataset achieved 90%,76%,84% sen,spec,accuracy
Koh et al 2021[18]	Steerable Pyramid Transform for feature analysis and adaptive synthetic sampling	Biopsy images with 2 sets. N= 31 and N= 46	10 fold cross validation	Senitivity 89.67%,Specificity 86.67% ,Accuracy 88.89% .
Molder et al 2023 [17]	CNN is compared with 3 ML algorithms: WKNN, Bagged tree, and Boosted tree.	Endoscopy images 66 CD and 16 Normal with 397 training patches and 170 testing patches	Train split validation(no cross validation)	99.30 sensitivity, 98.24 % accuracy, 98.61% PPV and 96.15% NPV
Zhou et al 2017 [19]	Deep CNN	VCE CD=11 frame Normal =10	7-fold cross validation	100% sensitivity.100% specificity
Ciaccio et al 2019[20]	Using basis image and non linear discriminant feature	VCE CD=13 Normal=13	8 basis images constructed for each image	84.6% sensitivity, 92.3% specificity
Manas Minnoor [21]	Random forest Algorithm	569 images of breast cancer	5 fold cross validation	100% accuracy
Wang et al 2020 [22]	ResNet 50 and inception V3 and classification done on soft-max, LDA, SVM and KNN	VCE CD=52 Normal=55	10-fold cross validation	Accuracy 95.94%, Sensitivity 97.20% and specificity 95.63%
Kwitt et al 2014 [24]	Fisher vector, binary pattern and dual tree for feature extraction and SVM for classification	EGD	50-fold Cross validation	92.0% accuracy, 97.5% sensitivity, 90.0% specificity
Vichensh et al 2019 [23]	Daisy descriptor, Shannon entropy And PSO	VCE CD=52 Normal 55	10-fold cross validation	89.82% accuracy, 94.35% sensitivity, 83.20% specificity
Saken et al 2021[32]	Context based multilevel thresholding and DWT	EGD 1661 images	-	94.79% accuracy, 94.29% sensitivity, 95.09% specificity

MATERIAL AND METHOD

The patients suspected of CD according to the test by serology(IgA-TTG and IgG-TTg) followed by upper GI endoscopy with biopsy are considered for the observation in this study.[17] Histopathology results are also reported for biopsy samples according to Marsh Oberhuber classification.[27] The Marsh 3 grading is done for mucosal injury in duodenum and non-CD patients are given Marsh 0-1 classification. The images of endoscopy are selected before the biopsy sample is taken. The patients with uncertainty in diagnosis are not taken in this study. Images are transferred by deidentifying for further image processing. All patients signed consent forms for using medical data and de-identifying endoscopy images for research purposes. As the dataset is small, so no cross-validation is performed.[28] We have just trained the images and then validated them with the help of endoscopists.

DATA ACQUISITION

The experimental data set was obtained from Olympus flexible endoscope EVIS EXERA III (GIF-H190) which was interpreted by an experienced gastroenterologist at PGIMS, Rohtak, India. The primary data is taken as online data is not available for manual endoscopy images. The endoscopy images are taken through an Olympus endoscope (GIF H-190) with an outer diameter of 9.2 mm having a narrow band imaging facility to view double the distance as captured through old scopes and enhance visualization of mucosal morphology.

The patients have been fasting since morning and the flexible endoscope tube with the camera pointed at the tip is inserted through the mouth, which travels through the esophagus, stomach, and small intestine which is also known as duodenum. The camera captures multiple images of duodenum folds for normal and celiac disease patients. The dataset contains 266 images of patients with damaged villi and 78 images with healthy villi. Seven patient's images are shown in Table 2 which contains grading and region by viewing through endoscope given by experts. Normal patients have no grading. There are 26 celiac patients and 15 normal patients The size of each raw image is 640 x 480 pixels. The images captured through the endoscope are sometimes blurry as the patient suffers from the pain as it passes through the GI(gastrointestinal) tract. The light conditions are also poor inside the body so we get low-contrast images.

IMAGE PROCESSING TECHNIQUES

Pre-processing

To resize images to a uniform resolution, normalize pixel values to a common scale, remove noise from raw data, and convert images to grayscale for simplicity and computational efficiency, preprocessing of raw data is an essential step.[29] Resizing also helps reduce computational complexity and memory requirements during model training, facilitating faster convergence and improved efficiency. The original size of the image is 640 x 480 pixels and resizing converts the size into 320 x 320 pixels. Then for denoising, the fastNLmeans denoising algorithm is used. It is different from the local mean method like Gaussian blur as it takes the mean value of all the similar pixels related to the target pixel that are present in the image rather than taking the mean value of the surrounding pixel for the target image. In this study, SMOTE (Synthetic Minority Over-sampling Technique) is used to address class imbalance in the dataset. SMOTE generates synthetic samples for the minority class to balance class distribution. Here minority class refers to normal images and it is increased to 159 images. So, now the dataset contains (266,159) images, and out of 425 images 340 images are used in training and 85 images in testing as shown in Figure 2 by partitioning into 80 and 20 ratios.[30]

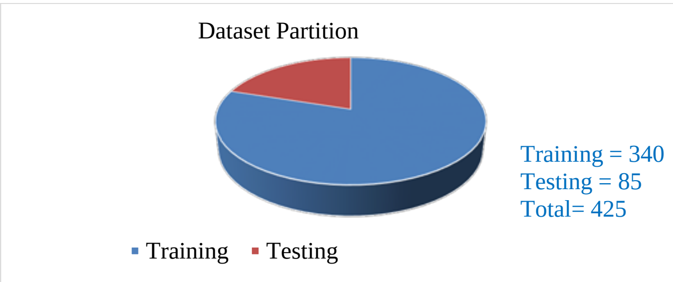

Figure 2: Dataset partition

Segmentation

In this paper, we have applied automated detection on segmented images. Segmentation is the process of finding the particular region of interest for the ease of classification in the next stage. A few years back it was not so popular as the researcher went for classification after extracting features from the preprocessed image. But nowadays it is quite popular in the medical field. After preprocessing, the particular region of interest (ROI) is labeled. Various methods are used for finding ROI like thresholding, region-based, edge detection, and some hybrid approach by mixing two methods. The Sobel operator is used in finding edge information in two horizontal and vertical directions. Some methods convert the picture in foreground and background for calculating the entropy known as Kapur entropy.[31]

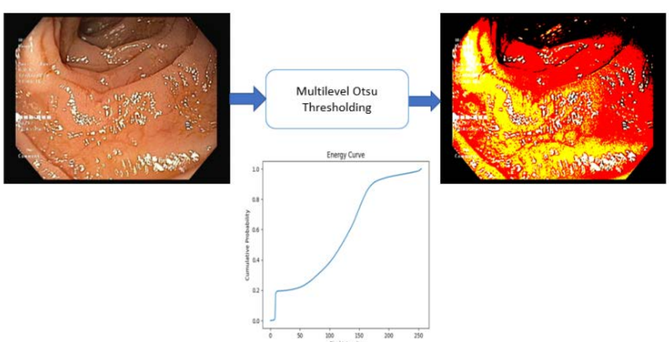

Figure 3: Multilevel Otsu thresholding approach with energy curve

Otsu's method computes one best threshold to separate an entire picture into two parts: one with a white background and another with a black foreground. However, this research aims at an extension called Multi-Otsu thresholding where several such thresholds can be computed simultaneously so that many distinct regions are obtained depending on some distribution local characteristics. To implement this, a segmentation model was designed on the hybrid approach of multilevel otsu thresholding with a Sobel operator, avoiding the disadvantages mentioned above.[32] To convert the image into a binary image called binarization, the gray level value is to check the threshold limit if it is greater than some set value then it returns 1 otherwise 0.[33,34] Figure 3 shows the optimal multilevel Otsu thresholding stage for finding various thresholds based on the intensity value.

Feature extraction

After finding a particular ROI, the next stage is to find a feature vector to define an appropriate class. Wavelet transforms have been used in classification of the celiac disease for a long time.[35–37] Here, after segmentation discrete wavelet transform (DWT)[38] is applied for transforming images into wavelets with high and low pass filters with four coefficients namely approximation, diagonal, vertical, and horizontal. This decomposition is applied on the segmented images up to 3 levels of decomposition to achieve better accuracy. The four subbands LL, LH, HL, and HH are visible after 3rd level. For extracting the best feature DWT is combined with HOS(high order spectra). Other feature extraction methods LBP (Local binary pattern) and HOG(Histogram of oriented gradient) are also applied but the hybrid approach of DWT-HOS gives better performance in extracting spatial information. The LBP method is mostly used in the classification of intestine diseases like celiac, and Crohn's disease. Here texture features are determined by calculating the difference of neighboring pixels. The result of LBP extraction is a feature vector that represents the distribution of different local patterns in the image. It provides information about texture patterns, such as edges, corners, and flat areas. The LBP algorithm parameters with N points =8, 32 cell sizes, and radii = 1. HOG is a feature descriptor used for object detection and recognition in computer vision. It represents the distribution of gradient orientations in localized portions of an image. The result of HOG extraction is a feature vector that captures the shape and appearance of objects based on their gradient orientation information.

HOS: HOS features are derived from the spectrogram of the image, capturing higher-order statistical information beyond mean and variance. In this context, it appears that HOS features are extracted from the wavelet-transformed subbands of the image. The result is a feature vector representing the higher-order statistical properties of the image, which can be used for various purposes such as classification or analysis of signal characteristics. In our implementation, we calculate HOS features from spectrograms of wavelet subbands, which involve complex mathematical operations on the image data. DWT HOS combines the Discrete Wavelet Transform (DWT) with Higher Order Statistics (HOS) computed from spectrograms of DWT subbands. It aims to capture the statistical characteristics of the wavelet coefficients. Spectrograms are computed for each subband, and HOS features are extracted from them. The resultant HOS feature vector for each subband is concatenated to form the final feature vector.

Classification

Random forest (RF) is an ensemble machine-learning algorithm that combines the prediction of different trees to find out the average to enhance the performance of the model. Each decision tree in the ensemble is trained on a random subset of the training data and a random subset of features. During prediction, each tree in the ensemble predicts the class label and the final prediction is determined by a majority vote among all.[30,39] This concludes in two steps: Combine all the trees in the first stage and then give a prediction for each tree in the second stage.[40] In this work, a Balanced Random Forest Classifier is used. This classifier is specifically designed to handle imbalanced datasets by adjusting class weights during training. Minority class is given higher weights and majority class images are given lower weights, thereby reducing bias towards the majority class. Hyperparameters are used in classification to fine-tune the model's performance. In this work, the 'n-estimators' hyperparameter is used to specify the number of decision trees in the Random Forest Classifier. 'n-estimators=100' specifies the number of decision trees in the Random Forest Classifier. In this case, the classifier ensemble consists of 100 decision trees. SMOTE framework that we integrate with the Random Forest (RF) architecture to benefit from the power of the ensemble and obtain better generalization.

Table 2: Real dataset image description by endoscopist

Image	Type	Region	Grading Pathology reports
	Abnormal Attenuated folds	In left	Marsh3a
	Abnormal Loss of folds	Upside	Marsh 3a
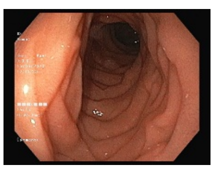	Normal	No flattening	Marsh 0
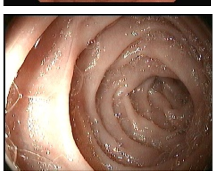	Normal	No flattening	Marsh 0
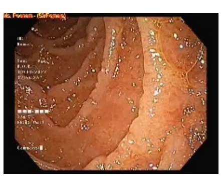	Abnormal Scalloping	Right side in maximum folds	Marsh 3b
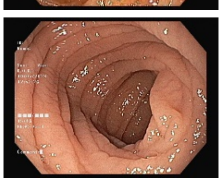	Abnormal Scalloping	Partial folds	Marsh 3a
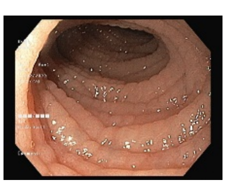	Abnormal Scalloping	All the folds	Marsh 3c (high severity)

Result

This section introduces the performance measures of the Balanced random forest classifier, which was implemented using Python 3.11.3 version. A total of 41 patients are considered for the analysis with 26 patients CD and 15 patients normal. All diseased patients have villous atrophy and positive serology tests while the normal patients have normal mucosa and negative serology reports. Suspected patients are not included in this study. A total of 266 images are taken from CD patients and 78 images from normal patients. SMOTE is used to increase the minority class with a ratio of 0.6 resulting in a final dataset of (266,159) images. The data is divided into the ratio of 80% training and 20% testing. The diagnostic performance was calculated for the machine learning algorithm and validated with manual segmentation. The parameters precision, recall, F1 score, and accuracy are considered for model performance.[41] The high value of precision achieved indicates that the model has a low false positive rate and is effective at correctly identifying positive instances. Accuracy calculates how many images are correctly classified among all positive and negative instances. While accuracy provides a general measure of the performance of the model, its performance can be ambiguous in the case of the imbalanced dataset. The model achieves a precision of 94.23 %, recall of 89.09 %, 89.41 % accuracy, and F1 score of 91.58 % for abnormal (celiac) images. Table 3 gives parameters achieved through the Balanced Random Forest Classifier.

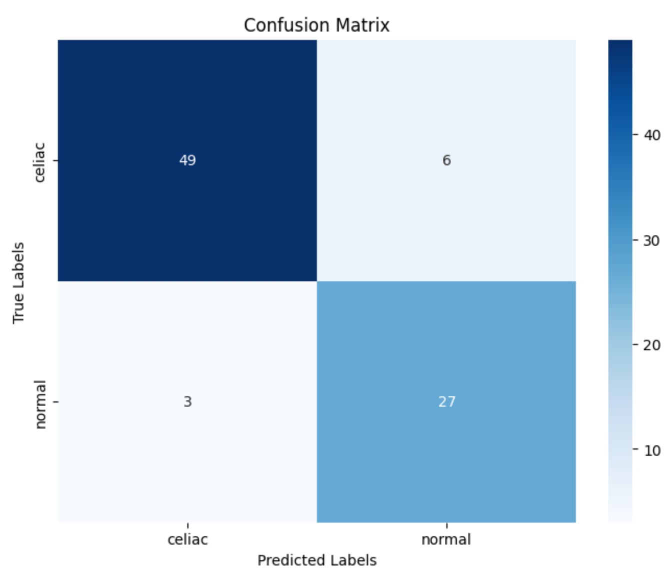

Figure 4: Confusion matrix

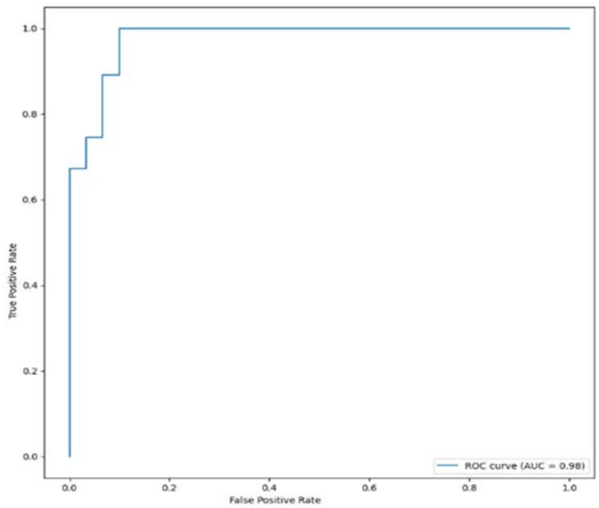

Figure 5: ROC curve

Table 3: Results of classification using a Balanced random forest classifier

S. No	Para meters	Abnormal (%)	Normal (%)	Formula
1	Precision	94.23	81.81	$\frac{TP}{TP+FP}$
2	Recall	89.09	90.0	$\frac{TP}{TP+FN}$
3	F1score	91.58	85.70	$2\times\frac{P\times R}{P+R}$
4	Accuracy	89.41	89.41	$\frac{TP+TN}{Total}$
5	Misclassification rate	10.58	10.58	$\frac{FP+FN}{Total}$

Here Total = TP+FP+TN+FN. It can be observed from Table 3 that the Balanced random forest (RF) algorithm outperforms for majority dataset than manual classification by imparting high precision and accuracy. Here P stands for precision and R stands for recall.

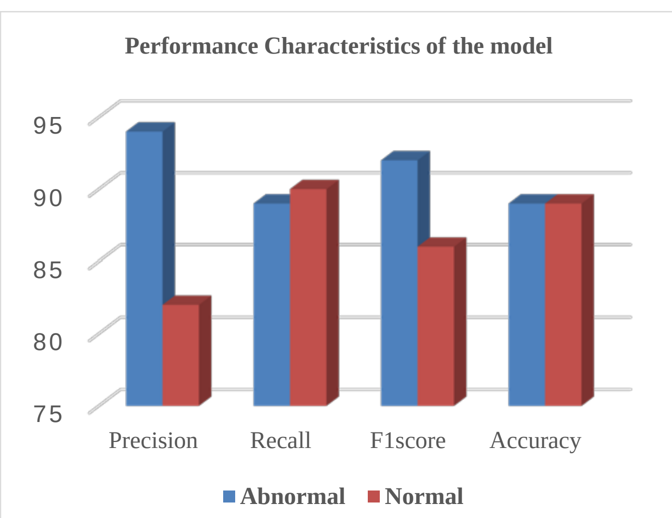

Figure 6: Performace measure of the model

Figure 4 gives the confusion matrix obtained through the model. This matrix gives values of true positive, true negative, false positive, and false negative cases. With the help of this matrix, we can calculate different parameters. The ROC curve is used to estimate the performance of the model. The higher the AUC value better the model classifies the two classes.[42] The receiver operating characteristics for an AUC score of 0.98 is shown in Figure 5.

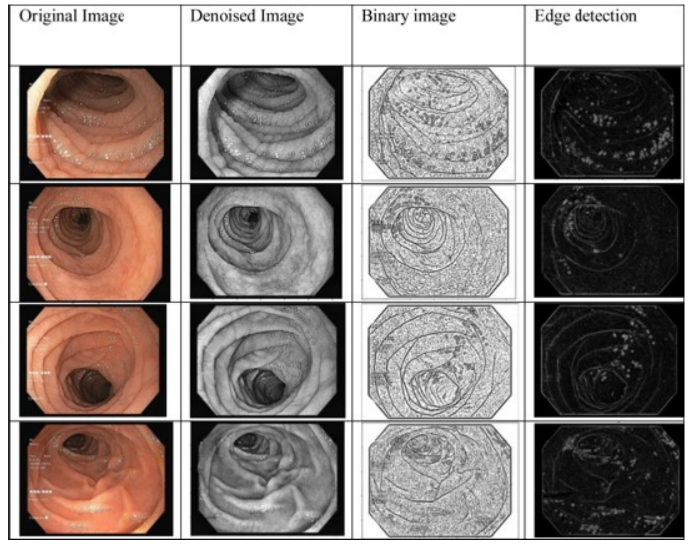

Figure 7: Results Analysis of various stages of image processing for different celiac images

Figure 6 gives parameters evaluation of different metrics in the form of a bar graph given in Table 3 and Figure 7 gives various stages of image processing techniques implemented on the celiac images (a) original image (b) Denoised image with the help of Gaussian blur (c) Binarization (d) Segmented image for particular ROI

Discussion

The mucosa injury due to celiac disease recovers after taking gluten gluten-free diet. Due to various pitfalls in histology, interest in computer-based diagnosis has increased for adult patients of CD for accurate diagnosis of villous atrophy. The AI algorithms also help in targeting the diseased area from where the biopsy sample should be taken due to the patchy nature of VA. This patchy nature can occur in another disease other than celiac. So, detection of VA is not a compulsion of having celiac disease. The biggest limitation is that AI learns through observation and provides good outcomes with data similar to what they are trained in. If data is small and from one specific source then generalized behavior can not be seen. So, validation on large datasets and controlled CD, tests on different endoscopy devices, and chromoendoscopy images is also necessary. The images captured are limited to time restrictions, as endoscopy was not done only for CD patients specifically. The serology and pathology reports are also taken to evaluate the ground truth image. The cost-effective SMOTE-RF approach is more effective than complex approaches like CNN for small datasets. DWT-HOS feature extraction can extract features for classification with high accuracy. It has also been observed that a cost-effective

SMOTE-RF approach with gradient magnitude and multi-otsu segmentation provides novelty to the work in the case of a small dataset.

Conclusion and future scope

The gold standard method of endoscopy for diagnosis depends mainly on the observer, so in this study hybrid approach is used for the classification of the disease. The results achieved show that the cost-effective BRF method is efficient for the classification of the disease. Random Forest classifier is effective in classifying medical images because they are strong, and perform tasks easily with imbanced datasets. So, better diagnoses, treatment, and care of patients on time due to detection at an early stage. The energy-multilevel Otsu thresholding method segments the images based on the energy intensity of the pixel. DWT-HOS feature extraction with SMOTE-Balanced random forest classifier approach achieves an accuracy of 89.41%, precision of 94.23%, recall of 89.09%, and F1 score of 91.58%. The results of this hybrid approach show the efficacy of the model by validating the segmented images with a doctor, as a comparison can not be performed for this kind of dataset. In the future, accuracy can be further improved by increasing the dataset and implementing a new hybrid classification approach for better and early diagnoses within less complex approaches for effective results.

Conflict of interest

All the authors declare no conflict of interest.

Acknowledgment

Authors thank Dr Sandeep Goyal, Professor and Head, Department of Gastroenterology and Medicine, PGIMS, Rohtak for timely help in understanding of endoscopy images and segmenting the images.

Author contributions

Nisha: Conceptualization, Methodology, Data collection, Paper writing, analysis and interpretation of results. Prachi Chaudhary: Conceptualization, Methodology, Visualization, Writing-Reviewing and Editing

References

1. I. Parzanese, D. Qehajaj, F. Patrinicola, et al. Celiac disease: From pathophysiology to treatment. *World J. Gastrointest. Pathophysiol.* **2017**, 8 (2), 27.
2. S. 'Guandalini, A. 'Assiri. Celiac disease: a review. *JAMA Pediatr* **2014**, 168 (3), 272–278.
3. P. Singh, A. Arora, T.A. Strand, et al. Global Prevalence of Celiac Disease: Systematic Review and Meta-analysis. *Clin. Gastroenterol. Hepatol.* **2018**, 16 (6), 823–836.e2.
4. S.D. Johnston, R.G.P. Watson, S.A. McMillan, J. Sloan, A.H.G. Love. Prevalence of coeliac disease in Northern Ireland. *Lancet* **1997**, 350 (9088), 1370.
5. L.E. White, V.M. Merrick, E. Bannerman, et al. The rising incidence of celiac disease in Scotland. *Pediatrics* **2013**, 132 (4).
6. F. Cataldo, G. Montalto. Celiac disease in the developing countries: A new and challenging public health problem. *World J. Gastroenterol.* **2007**, 13 (15), 2153–2159.
7. V. 'Khoshoo, "Bhan M K", et al. Coeliac disease as cause of protracted diarrhoea in Indian children. *Lancet* **1988**.
8. P. Singh, S. Shergill, G.K. Makharia. Celiac disease in older adults. *J Gastrointestin Liver Dis* **2013**, 22(3), 359.
9. P. Chaudhary, Nisha. Comparative Analysis of Techniques used for Detection of Celiac Disease using Various Endoscopies. *Int. J. Adv. Res. Eng. Technol.* **2020**, 11 (12), 1521–1529.
10. M.W. Scheppach, D. Rauber, J. Stallhofer, et al. Detection of duodenal villous atrophy on endoscopic images using a deep learning algorithm. *Gastrointest. Endosc.* **2023**, 97 (5), 911–916.
11. W. 'Dickey, D. 'Hughes. Disappointing sensitivity of endoscopic markers for villous atrophy in a high-risk population: implications for celiac disease diagnosis during routine endoscopy. *Am J Gastroenterol* **2001**, 96 (7), 2126–2128.
12. M. Owais, M. Arsalan, J. Choi, T. Mahmood, K.R. Park. Artificial intelligence-based classification of multiple gastrointestinal diseases using endoscopy videos for clinical diagnosis. *J. Clin. Med.* **2019**, 8 (7).
13. K. Doi. Computer-Aided Diagnosis in Medical Imaging: Historical Review, Current Status and Future Potential. *Comput. Med. Imaging Graph.* **2007**, 31 (4–5), 198–211.
14. G. Varoquaux, V. Cheplygina. Machine learning for medical imaging: methodological failures and recommendations for the future. *NPJ Digit. Med.* **2022**, 5 (1), 48.
15. R. Sujatha, J.M. Chatterjee, N.Z. Jhanjhi, S.N. Brohi. Performance of deep learning vs machine learning in plant leaf disease detection. *Microprocess. Microsyst.* **2021**, 80.
16. R. Bisschops, M. Areia, E. Coron, et al. Performance measures for upper gastrointestinal endoscopy: A European Society of Gastrointestinal Endoscopy (ESGE) Quality Improvement Initiative. *Endoscopy* **2016**, 48 (9), 843–864.
17. A. Molder, D.V. Balaban, C.C. Molder, M. Jinga, A. Robin. Computer-Based Diagnosis of Celiac Disease by Quantitative Processing of Duodenal Endoscopy Images. *Diagnostics* **2023**, 13 (17).
18. J.E.W. Koh, S. De Michele, V.K. Sudarshan, et al. Automated interpretation of biopsy images for the detection of celiac disease using a machine learning approach. *Comput. Methods Programs Biomed.* **2021**, 203.
19. T. Zhou, G. Han, B.N. Li, et al. Quantitative analysis of patients with celiac disease by video capsule endoscopy: A deep learning method. *Comput. Biol. Med.* **2017**, 85, 1–6.
20. E.J. Ciaccio, C.A. Tennyson, G. Bhagat, S.K. Lewis, P.H. Green. Use of basis images for detection and classification of celiac disease. *Bio-Medical Materials and Engineering*; **2014**, 24(6), 1913–1923.
21. M. Minnoor, V. Baths. Diagnosis of Breast Cancer Using Random Forests. In *Procedia Computer Science*; Elsevier B.V., **2022**; Vol. 218, pp 429–437.
22. X. Wang, H. Qian, E.J. Ciaccio, et al. Celiac disease diagnosis from video capsule endoscopy images with residual learning and deep feature extraction. *Comput. Methods Programs Biomed.* **2020**, 187.
23. J. Vicnesh, J.K.E. Wei, E.J. Ciaccio, et al. Automated diagnosis of celiac disease by video capsule endoscopy using DAISY Descriptors. *J. Med. Syst.* **2019**, 43 (6).
24. Y.Y. Zhao, D.X. Xue, Y.L. Wang et.al. Computer-assisted diagnosis of early esophageal squamous cell carcinoma using narrow-band imaging magnifying endoscopy. *Endoscopy*, **2019**, 51(04), 333-341.
25. V. Jackins, S. Vimal, M. Kaliappan, M.Y. Lee. AI-based smart prediction of clinical disease using random forest classifier and Naive Bayes. *J. Supercomput.* **2021**, 77 (5), 5198–5219.
26. A. Sarica, A. Cerasa, A. Quattrone. Random forest algorithm for the classification of neuroimaging data in Alzheimer's disease: A systematic review. *Frontiers in Aging Neuroscience*. 2017, 9, 239.
27. G. 'Oberhuber, G. 'Granditsch, H. 'Vogelsang. The histopathology of coeliac disease: time for a standardized report scheme for pathologists. *Eur J Gastroenterol Hepatol* **1999**, 11 (10), 1185–1194.
28. P. Burman. A comparative study of ordinary cross-validation, v-fold cross-validation, and the repeated learning-testing methods. *Biometrika* **1989**, 76 (3), 503–514.
29. Nisha, P. Chaudhary. Denoising the Endoscopy Images of the Gastrointestinal Tract Using Complex-Valued CNN. In *Lecture Notes in Networks and Systems*; Springer Science and Business Media Deutschland GmbH, **2024**; Vol. 785, pp 439–448.

30. S. Patil-Kashid, Y.M. Patil, A. Kashid. Facial expression recognition for wild dataset using LBP features and Random Forest Classifier. *J. Integr. Sci. Technol* **2024**, 2024 (5), 817.
31. J.N. 'Kapur, P.K. 'Sahoo, A.K.C. 'Wong. A new method for Gray level Picture Thresholding Using the Entropy of the Histogram. *Comput. Vis. Graph. Image Process.* **1985**, 273–285.
32. M. Saken, M. Banzragch Yağci, N. Yumuşak. Impact of image segmentation techniques on celiac disease classification using scale invariant texture descriptors for standard flexible endoscopic systems. *Turkish J. Electr. Eng. Comput. Sci.* **2021**, 29 (2), 598–615.
33. S. Khairnar, S.D. Thepade, S. Gite. Effect of image binarization thresholds on breast cancer identification in mammography images using OTSU, Niblack, Burnsen, Thepade's SBTC. *Intell. Syst. with Appl.* **2021**, 10 (11), 46.
34. B.M. Rashed, N. Popescu. Performance Investigation for Medical Image Evaluation and Diagnosis Using Machine-Learning and Deep-Learning Techniques. *Computation* **2023**, 11 (3).
35. M. Gadermayr, M. Liedlgruber, A. Uhl, A. Vécsei. Evaluation of different distortion correction methods and interpolation techniques for an automated classification of celiac disease. *Comput. Methods Programs Biomed.* **2013**, 112 (3), 694–712.
36. A. Vecsei, T. Fuhrmann, M. Liedlgruber, L. Brunauer, H. Payer, A. Uhl. Automated classification of duodenal imagery in celiac disease using evolved fourier feature vectors. *Computer methods and programs in biomedicine*, **2009**, 95(2), S68-S78.
37. A. Rehman, Y. Gao, J. Wang, Z. Wang. Image classification based on complex wavelet structural similarity. *Signal Processing: Image Communication*, **2013**, 28(8), 984-992.
38. J.P. Antoine, P. Carrette, R. Murenzi, B. Piette. Image analysis with two-dimensional continuous wavelet transform. *Signal processing*, **1993**, 31(3), 241-272.
39. A. Subudhi, M. Dash, S. Sabut. Automated segmentation and classification of brain stroke using expectation-maximization and random forest classifier. *Biocybern. Biomed. Eng.* **2020**, 40 (1), 277–289.
40. N. Amini, A. Shalbaf. Automatic classification of severity of COVID-19 patients using texture feature and random forest based on computed tomography images. *Int. J. Imaging Syst. Technol.* **2022**, 32 (1), 102–110.
41. R. Patil, V. Raut, S.A. Shirsat, et al. Securing Visual Integrity: Machine learning approaches for forged image detection. *J. Integr. Sci. Technol* **2024**, 12(5), 815.
42. G. Pole, P. Gera. Combined clustering with classification in a semi-supervised context: An efficient data partitioning. *J. Integr. Sci. Technol* **2024**, 12(5), 824.